

Original Article



A Temporal Dynamic Assessment of Eco-environmental Quality in Guangxi, China (2000–2020), Based on GEE and RSEI

Yu Bai¹, Xiangling Tang^{1,*}, Wei Li¹, Tingjiang Tan¹, Xuemei Zhong¹, Dujiang Long²

¹College of Earth Sciences, Guilin University of Technology, Guilin 541004, China

²Guangxi Ecological Environment and Landscape Protection Research Center, Guilin Tourism University, Guilin 541004, China

*Corresponding Author: Xiangling Tang

Abstract:

As a representative ecologically vulnerable zone, Guangxi Zhuang Autonomous Region necessitates systematic quantification of spatiotemporal eco-environmental dynamics to inform conservation governance. Leveraging Google Earth Engine (GEE), this research constructed a MODIS-derived Remote Sensing Ecological Index (RSEI), supplemented by spatial autocorrelation diagnostics to decode change patterns. The findings demonstrate that: (1) the average RSEI values across the years 2000, 2005, 2010, 2015, and 2020 were 0.677, 0.663, 0.782, 0.741, and 0.767, respectively, suggesting a declining trend in ecological quality during 2000–2005, followed by an overall improvement from 2010 to 2020. (2) LISA cluster mapping revealed predominant high-high (H-H) aggregations in the study area's northeastern sector, contrasting with concentrated low-low (L-L) clusters encircling Nanning and territories contiguous to Guangdong Province. (3) From 2000 to 2020, the area classified as "Critical" decreased by 303.5 km², "Suboptimal" areas declined by 4,108 km², "Marginal" areas by 26,178.25 km², and "Acceptable" areas by 49,679.5 km², while "Optimal" areas increased by 79,859.75 km², indicating an overall shift toward higher ecological quality. (4) Elevation and slope were found to be the most crucial factors affecting RSEI changes from 2000 to 2020.

Keywords: RSEI; GEE; Spatiotemporal Variation; Ecological Environment Quality

1. Introduction

Reflecting the integrated configuration of ecosystems and their components, the ecological environment forms a complex socio-economic-natural composite system. As the foundational substrate for human survival and development, it intrinsically links to livelihood security and sustainable societal advancement. Rapid urbanization, intensifying anthropogenic pressures, and resource overexploitation have triggered ecological degradation at regional-to-global scales. Ecological perturbations in densely populated urban centers compromise terrestrial ecosystem services while directly threatening human welfare and sustainability trajectories [1-3]. Echoing these challenges, China's 14th Five-

Year Plan codifies "ecological priority and green development" as core tenets. Consequently, vigilant monitoring of spatiotemporal eco-environmental quality patterns becomes imperative for enhancing environmental governance, informing spatial planning, and achieving sustainable development objectives [4].

Owing to its remarkable advantages such as high timeliness, strong periodicity, and extensive coverage, remote sensing technology has been extensively utilized in the field of ecological and environmental assessments. The existing methodologies can be generally classified into two distinct categories. The first relies on single-indicator analysis [5-6]; however, given the

multifactorial nature of ecosystems, such methods are often insufficient to comprehensively represent regional ecological quality. The second type integrates multiple indicators, with the most representative being the Remote Sensing Ecological Index (RSEI) [7], which has been recognized for its objectivity and comprehensiveness applied at various administrative scales [8-9]. Some scholars, considering the temporal limitations of Landsat time series data, have adopted time intervals of 5 to 10 years for RSEI construction [10–11], which limits the ability to capture subtle year-to-year changes. MODIS data, with its broad spatial coverage and continuous time series, has become a preferred source for constructing RSEI for ecological evaluations at provincial or national scales [12]. Processing and analyzing voluminous remote sensing datasets impose significant constraints on data acquisition and computational resources. Google Earth Engine (GEE) overcomes these limitations through integrated cloud computing and massive data storage, proving particularly effective for large-scale, long-term ecological monitoring. Its application in multi-scale ecological assessments is well-documented [13–15]. Crucially, GEE hosts preprocessed datasets (e.g., Landsat series) including top-of-atmosphere (TOA) and surface reflectance products, bypassing complex radiative transfer corrections [16]. This renders GEE superior to conventional tools for regional RSEI development and ecological quality evaluation.

As a regionally representative karst terrain in China, Guangxi Zhuang Autonomous Region manifests mild climatic regimes and optimal thermohydrological conditions. Its extensive vegetation coverage underpins exceptional ecological significance, functioning as a vital national agricultural base and ecological security buffer. However, due to poor soil-forming material, suboptimal site conditions for vegetation, high ecological sensitivity, and significant human-environment conflicts, Guangxi

is recognized as a typical ecologically fragile region [17]. While some studies have assessed ecological quality in karst areas, most focus on local sub-regions, lacking comprehensive regional-scale analyses [18–19]. Consequently, this research operationalizes the GEE platform to generate quinquennial RSEI assessments for Guangxi (2000-2020), decoding spatiotemporal trajectories and mechanistic drivers of ecological quality evolution. These findings establish an empirical foundation for advancing SDG-aligned regional development through sustainable resource governance.

2. Materials and Methods

2.1. Study Area Overview

As illustrated in Figure 1, the Guangxi Zhuang Autonomous Region, located in the southern part of China, spans a longitudinal range from 104°26' to 112°04'E and a latitudinal range from 20°54' to 26°24'N. Bounded by the Nanling Mountains in the north and the Beibu Gulf in the south, its northwestern part is situated on the southeastern margin of the Yunnan–Guizhou Plateau, forming a significant geological transition zone that connects the plateau with the hilly terrain of the southeastern coastal region. The topography generally descends from the western, northwestern, and northeastern sectors towards the central and southeastern portions of the region. Topographically, the region is higher along the periphery and lower in the center, resembling a basin. The landscape is characterized by continuous mountain ranges, undulating hills, limited plains, numerous rivers, and widespread karst formations. The climate of Guangxi falls under the categories of mid-subtropical and south-subtropical monsoon climates. It is marked by synchronized rainfall and heat, with uneven spatiotemporal distribution of precipitation. Summers are long, hot, and humid with abundant rainfall, while winters are short, dry, and relatively warm.

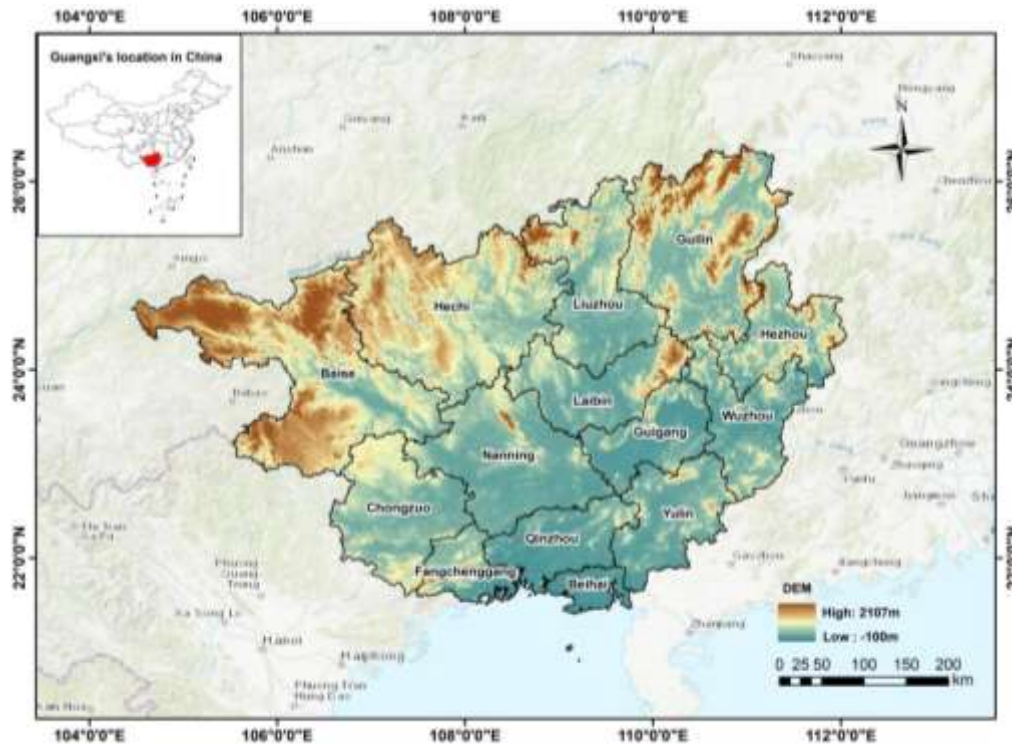


Figure 1. Geographical location of Guangxi Zhuang Autonomous Region in China.

2.2. Data Sources

Specifically covering the period from June to September, remote sensing data, particularly MODIS product data for the years 2000, 2005, 2010, 2015, and 2020, were acquired from the

Google Earth Engine (GEE) platform. Table 1 presents detailed information in a comprehensive manner.

Table 1. Description of remote sensing data products used in this study.

Data Product	Data Layer	Spatial Resolution (m)	Temporal Resolution (days)	Number of Scenes	Application
MOD13A1 V6	Vegetation Index (NDVI)	500	16	640	Greenness indicator
MOD11A2 V6	Land Surface Temperature (LST)	1000	8	1280	Heat indicator
MOD09A1 V6	Surface Reflectance (Bands 1–7)	500	8	1280	Wetness and dryness indicators

Acquired from the National Earth System Science Data Center at a spatial resolution of 1 km, meteorological data encompassing mean annual temperature and total precipitation during the period from 2000 to 2020 were obtained for comprehensive analysis. Official government yearbooks served as the source for population and GDP statistics spanning from 2001 to 2020. These socioeconomic datasets were converted to 1 km raster format using spatial interpolation techniques. To ensure spatial consistency, a 30-m

Digital Elevation Model (DEM) sourced from the Geospatial Data Cloud (SRTM product) was resampled to a resolution of 1 km. The Resource and Environment Science and Data Center (RESDC, Chinese Academy of Sciences) provided land use classifications, which were then integrated into six standardized categories: cropland, forest, grassland, water bodies, built-up areas, and unused land. Through the application of the Modified Normalized Difference Water Index (MNDWI) for masking, to minimize the influence of water bodies on principal component loadings,

aquatic regions were deliberately excluded from the analysis.[20].

2.3. Research Method

2.3.1. Development of RSEI

The greenness component employs the Normalized Difference Vegetation Index (NDVI) as a proxy for vegetation vigor. Through the Tasseled Cap Transformation, moisture conditions are quantitatively assessed by means of the

wetness band (WET)[21], which captures surface and vegetation moisture. Land Surface Temperature (LST) serves as the heat component indicator. For the dryness component (NDSI), the normalized average is computed by integrating the Bare Soil Index (SI) and the Index-based Built-up Index (IBI), jointly capturing anthropogenic expansion and substrate desiccation. Mathematical formulations of these metrics are provided in Table 2.

Table 2. Calculation methods of RSEI component indicators.

Indicators	Calculation Methodology
NDVI	Extracted by MOD13A1
WET	$WET = 0.1147\rho_{Red} + 0.2489\rho_{NIR1} + 0.2408\rho_{Blue} + 0.3122\rho_{Green} - 0.3122\rho_{NIR2} - 0.6416\rho_{SWIR1} - 0.5087\rho_{SWIR2}$
LST	$LST = 0.02 \times D_N - 273.15$
NDSI	$NDSI = (SI + IBI) / 2$
	$SI = [(\rho_{SWIR1} + \rho_{Red}) - (\rho_{Blue} + \rho_{NIR})] / [(\rho_{SWIR1} + \rho_{Red}) + (\rho_{Blue} + \rho_{NIR})]$
	$IBI = \frac{2\rho_{SWIR1} / (\rho_{SWIR1} + \rho_{NIR}) - [\rho_{NIR} / (\rho_{NIR} + \rho_{Red}) + \rho_{Green} / (\rho_{Green} + \rho_{SWIR1})]}{2\rho_{SWIR1} / (\rho_{SWIR1} + \rho_{NIR}) + [\rho_{NIR} / (\rho_{NIR} + \rho_{Red}) + \rho_{Green} / (\rho_{Green} + \rho_{SWIR1})]}$

* Surface reflectance values correspond to specific MODIS bands.

* Grayscale values are derived from MOD11A2 imagery.

Following the normalization procedure, principal component analysis (PCA) was conducted on the integrated four component indicators to facilitate subsequent statistical evaluation. The initial Remote Sensing Ecological Index (RSEI₀) is

$$RSEI_0 = PC1[f(NDVI, WET, LST, NDSI)], \tag{1}$$

$$RSEI = \frac{RSEI_0 - RSEI_{0(\min)}}{RSEI_{0(\max)} - RSEI_{0(\min)}}, \tag{2}$$

In the given formula, the initial remote sensing ecological index is denoted by RSEI₀, while PC1 signifies the first principal component, and f represents the function of principal component analysis.

In order to enable comparisons across various time periods, the normalization of RSEI₀ to a range of 0 to 1 was performed, with higher values signifying superior ecological environment quality. For the purpose of enabling a more detailed evaluation, the RSEI indicators were divided into five distinct categories with intervals of 0.2: Critical (0–0.2), Su-

perior (0.2–0.4), Marginal (0.4–0.6), Acceptable (0.6–0.8), and Optimal (0.8–1.0).

2.3.2. Spatial Auto-correlation Analysis

Spatial autocorrelation serves as a critical measure for evaluating the interdependence between ecological environmental quality at a spatial unit and its adjacent areas [22]. This analytical approach facilitates the identification of spatial homogeneity or heterogeneity patterns in ecological conditions across the study region. Herein, local spatial autocorrelation metrics were

utilized to examine the spatial dependency structure of RSEI values[23].

Global Moran's I was used to quantify the overall spatial relationship among ecological indicators.

$$I = \frac{n}{S_0} \frac{\sum_{i=1}^n \sum_{j=1}^n W(i, j) (X_i - \bar{X})(X_j - \bar{X})}{\sum_{i=1}^n (X_i - \bar{X})^2}, \quad (3)$$

$$S_0 = \sum_{i=1}^n \sum_{j=1}^n W(i, j), \quad (4)$$

In the given equation, while n denotes the quantity of spatial units (study objects), X_i represents the observed value at location i, \bar{X} signifies the mean of all observed values, W indicates the aggregate of all spatial weights, and W_{ij} stands for the

$$Z(I) = \frac{1 - E(I)}{\sqrt{\text{var}(I)}}, \quad (5)$$

When examining spatial auto-correlation, it is noteworthy that $|Z(I)| > 1.96$ signifies significant spatial auto-correlation.

The Local Moran's I (LISA) statistic is an effective tool for capturing the spatial correlation of ecological environment quality among individual units within the study area. Each grid cell has its own local spatial auto-correlation

$$\text{Local Moran's } I = \frac{(D_i - \bar{D}) \times \sum_{j=1}^m W_{ij} (D_j - \bar{D})}{\sum_{i=1}^m (D_i - \bar{D})^2}, \quad (6)$$

The equation employs Local Moran's I as the local spatial autocorrelation metric, with computational parameters aligning.

For LISA map, it classifies the aggregation into 5 kinds of clusters. For H-H zones, both the focal site and its surroundings exhibit a high level of ecological quality. L-H clusters signify areas with locally depressed ecological quality surrounded by high-value regions, while H-L patterns reflect isolated high-quality areas embedded within low-performance surroundings.[27]

2.3.3. Driving Factors

Changes in RSEI are shaped by the intricate interaction between environmental factors and human actions [28]. In this study, while the RSEI

The value of this parameter varies within the range of -1 to 1, where greater absolute values suggest more pronounced spatial auto-correlation [24].

spatial weight between location i and location j as defined within the spatial contiguity matrix.

The result of the Moran's I is assessed by the following formula:

relationship [25], making the analysis of local spatial patterns particularly important. When global spatial auto-correlation is absent, LISA can help identify local clusters that may otherwise be obscured. Conversely, when global spatial auto-correlation is present, LISA can be used to assess spatial heterogeneity and pinpoint specific areas contributing to the global pattern [26]. The calculation formula is as follows:

values from 2000 to 2020 were utilized as the dependent variable, eight representative and accessible variables were chosen. The eight factors were considered as potential driving forces. Vegetation growth is significantly influenced by key environmental factors such as elevation, slope gradient, and precipitation patterns [29], where GDP, population density, and proximity to administrative centers indicate the intensity and scope of human activities [30].

The geographical detector serves as a spatial statistical tool for analyzing geographic heterogeneity and measuring the explanatory power of influencing factors[31–33]. In this study, the factor detector module was applied. This tool assesses the spatial heterogeneity of RSEI and

determines the extent to which a given factor (X)

explains the spatial variation in ecological quality.

$$q = 1 - \frac{\sum_{h=1}^L N_h \sigma^2}{N \sigma^2} = 1 - \frac{SSW}{SST}, \quad (7)$$

$$SSW = \sum_{h=1}^L N_h \sigma_h^2, SST = N \sigma^2, \quad (8)$$

Within the framework of stratified sampling, where $h=1, \dots, L$ represents the stratification or partition of variables or factors, N_h and N respectively denote the unit counts in stratum h and the entire domain. The median Y variances are expressed as σ_h^2 and σ^2 . SSW and SST represent within-stratum sum of squares and total sum of squares, respectively. The statistical metric q ($0 \leq q \leq 1$) quantifies the association strength between covariate x and response y , where elevated q values denote enhanced explanatory capacity.

3. Results

3.1. Comprehensive Assessment of Ecological Environment Quality in Guangxi

As illustrated in Table 3, among the five images from 2000 to 2020, the contribution rates of the first principal component (PC1) were 67.70%, 53.77%, 67.72%, 65.24%, and 71.42%, respectively. These results indicate that PC1 maintained a consistently dominant explanatory power for ecological environment quality across different years. This dominance suggests that PC1 can include the most of the ecological information, thereby accurately reflecting these overall ecological conditions in the Guangxi region. Further analysis of the component loadings revealed that PC1 primarily comprised

the NDVI and WET, both exhibiting positive loading values. These findings demonstrate that elevated vegetation coverage and improved moisture conditions enhance ecological quality. Conversely, negative loadings for Land Surface Temperature (LST) and the Normalized Difference Built-up and Soil Index (NDBSI) are key indicators in environmental studies. reveal that anthropogenic surface heating and wetland degradation degrade environmental integrity, consistent with established ecological principles. Based on the principal component contribution analysis, variations in the eigenvalues and contribution rates of PC1 demonstrate fluctuations in ecological environment quality across the evaluated years. Notably, the years 2000 and 2020 showed relatively high contribution rates, implying that ecological quality during these years was predominantly influenced by vegetation and moisture improvements, while the negative effects of temperature increase and wetland degradation gradually diminished.

Figure 2 illustrates the distribution characteristics and trends of the historical RSEI values in Guangxi from 2000 to 2020 based on five periods of RSEI images. The mean RSEI values were 0.677 (2000), 0.663 (2005), 0.782 (2010), 0.741 (2015), and 0.767 (2020), respectively.

Table 3. Principal component analysis results of RSEI in 2000, 2005, 2010, 2015, and 2020.

Year	Indicator(s)	PC1	PC2	PC3	PC4
2000	NDVI	0.995	0.075	-0.041	0.042
	LST	-0.045	0.894	0.438	-0.083
	WET	0.040	-0.351	0.809	0.469
	NDBSI	-0.073	0.268	-0.389	0.878
	Eigenvalue	0.019	0.007	0.002	0.000
	Percent eigenvalue	67.70%	22.88%	7.79%	1.63%
2005	NDVI	0.804	0.539	0.097	0.231
	LST	-0.163	0.183	0.936	-0.255
	WET	0.352	-0.766	0.327	0.427
	NDBSI	-0.451	0.298	0.091	0.837

	Eigenvalue	0.015	0.007	0.004	0.001
	Percent eigenvalue	53.77%	27.72%	13.32%	5.20%
2010	NDVI	0.979	-0.145	0.111	-0.086
	LST	-0.110	-0.965	-0.221	0.083
	WET	0.068	0.137	-0.833	-0.532
	NDBSI	-0.155	-0.168	0.496	-0.838
	Eigenvalue	0.012	0.004	0.001	0.000
	Percent eigenvalue	67.72%	24.04%	6.47%	1.76%
2015	NDVI	0.990	0.122	-0.017	0.064
	LST	-0.032	0.436	0.893	-0.109
	WET	0.064	-0.737	0.426	0.521
	NDBSI	-0.119	0.502	-0.146	0.844
	Eigenvalue	0.023	0.007	0.003	0.001
	Percent eigenvalue	65.24%	19.75%	10.65%	4.36%
2020	NDVI	0.991	-0.114	-0.059	0.033
	LST	-0.033	-0.659	0.751	0.035
	WET	0.028	0.361	0.277	0.890
	NDBSI	-0.125	-0.649	-0.597	0.453
	Eigenvalue	0.023	0.006	0.003	0.001
	Percent eigenvalue	71.42%	17.79%	8.43%	2.36%

From the perspective of overall trends, ecological environment quality in Guangxi improved gradually from 2000 to 2020, as indicated by the significantly increasing mean RSEI values, reaching 0.767 in 2020, suggesting a favorable ecological condition. Regarding the distribution characteristics, the lower quartiles of RSEI during the 2000–2020 period were consistently above 0.5, indicating that even regions with relatively poorer ecological conditions maintained a moderate to relatively good ecological status. The upper quartiles were consistently greater than 0.7, particularly prominent in 2010 and 2020. Moreover, the width of the boxplots was wider in 2000 and 2005, narrowing notably after 2010, suggesting that regional disparities in ecological quality have gradually decreased over time.

Considering critical years, the relatively lower RSEI values in 2000 and 2005 likely reflected widespread land development and urban expansion during that period, exerting notable pressure on ecosystems. A remarkable improvement occurred in 2010, as evidenced by a

mean RSEI reaching 0.782, with the upper quartile approaching 0.9, highlighting substantial achievements in ecological restoration and management during this period. The mean RSEI slightly declined in 2015 but rebounded to 0.767 in 2020, indicating a stable upward trend in overall ecological quality.

These results demonstrate that Guangxi's ecological environment quality was generally favorable, with mean RSEI values consistently ranging from 0.6 to 0.8, indicative of "good" to "excellent" ecological conditions. This reflects high vegetation coverage and favorable climatic conditions. Areas with lower ecological quality were primarily concentrated around economically developed urban regions, such as Nanning and its adjacent areas, which were strongly impacted by urbanization. Conversely, regions exhibiting higher ecological quality were mainly distributed across mountainous and hilly areas characterized by high forest coverage and relatively low human disturbance.

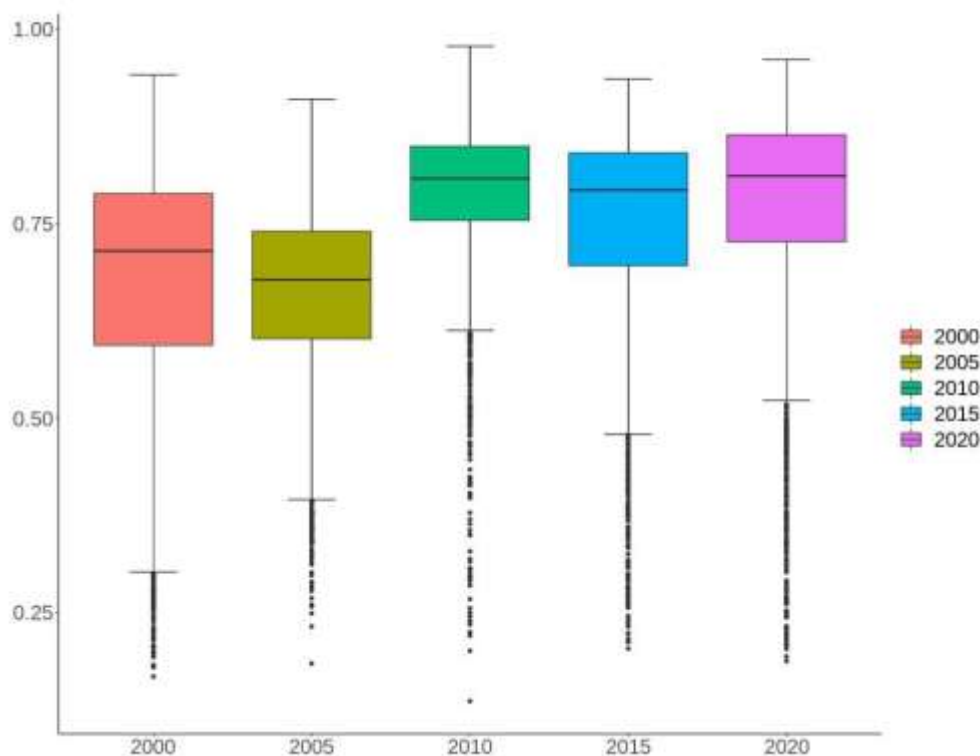


Figure 2. RSEI values in Guangxi from 2000 to 2020.

Spatio-temporal patterns in Guangxi's ecological environment quality (2000–2020) are presented in Figure 3, depicting regional classifications and variations. Within the figure, distinct color designations indicate ecological quality grades: red (Critical), orange (Suboptimal), yellow (Marginal), green (Acceptable), and blue (Optimal). Longitudinal analysis reveals that ecological conditions across Guangxi were consistently rated as 'good' throughout the study period. From a spatio-temporal perspective, areas characterized by critical and suboptimal ecological conditions were primarily concentrated in northern Guangxi and areas surrounding Nanning city. These regions have typically experienced intensive urbanization and human activities, leading to ecological degradation. Conversely, regions exhibiting acceptable and suboptimal ecological quality were predominantly located in the northwest and eastern parts of Guangxi, characterized by higher forest coverage, fewer human activities, and thriving ecosystems.

Regarding the ecological quality optimization trend during 2000–2020, ecological conditions in

2000 and 2005 were relatively poor, as evidenced by the larger proportions of red and orange areas, likely associated with urbanization and intensive land development practices. These practices presumably caused the deterioration of regional ecological environments due to excessive exploitation. After 2010, ecological quality significantly improved, indicated by the increasing coverage of green and blue areas, reflecting comprehensive improvements in forest coverage and water quality. From 2000 to 2020, there was a general trend of decreasing coverage of red and orange areas, accompanied by a corresponding increase in green and blue regions.

Overall, this analysis demonstrates a clear progression of Guangxi's ecological environment quality from moderate towards acceptable and optimal conditions. Areas exhibiting the most pronounced ecological improvements were concentrated primarily in the northwest and southeast. These findings provide critical insights and valuable support for environmental policy formulation and ecological optimization planning.

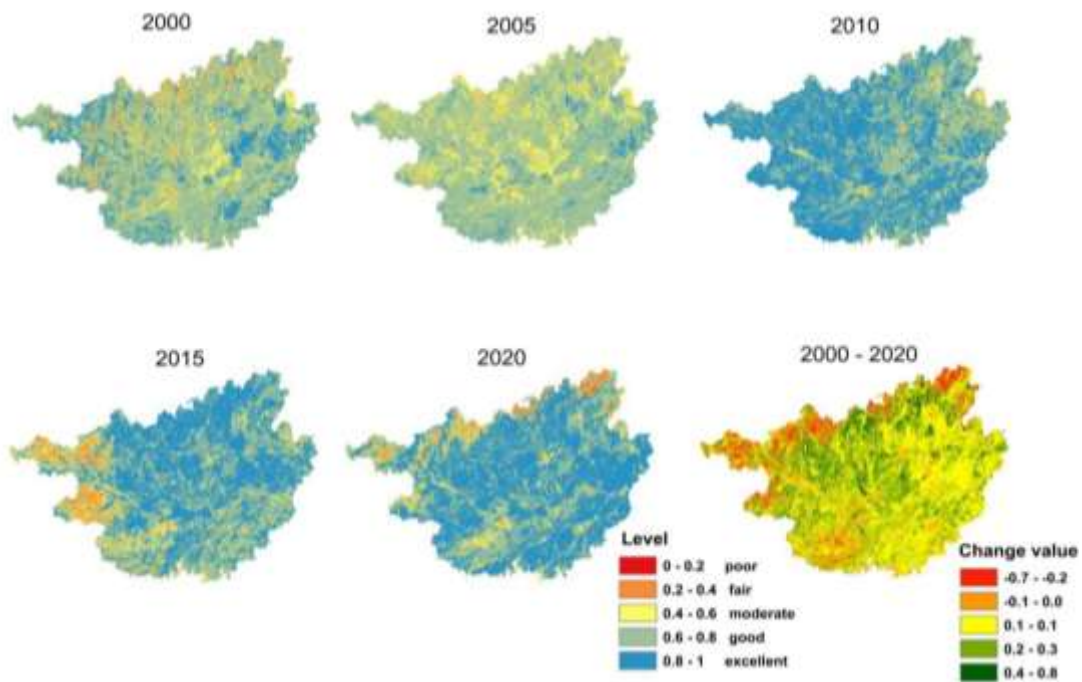


Figure 3. Spatio-temporal variations of RSEI.

Utilizing the RSEI maps for the years, the spatial extent and proportional distribution corresponding to each ecological quality category (critical, suboptimal, marginal, acceptable, optimal) were quantified. Figure 4 and Table 4 depict the temporal evolution of these categorical proportions over the 2000-2020 period. Notably, the aggregate proportion representing moderate, good, and excellent RSEI levels exhibited an upward trajectory. Conversely, the combined proportion attributed to poor and fair levels demonstrated a declining tendency. Detailed

categorical area and proportion data are compiled in Table 4.

Additionally, composite metrics were derived: the combined percentage for critical, suboptimal, and marginal levels (PFM%) and the combined percentage for Acceptable and Optimal levels (GE%). The calculated values were: 2000 (PFM%: 25.16%, GE%: 74.84%), 2005 (23.70%, 76.29%), 2010 (7.02%, 92.98%), 2015 (15.47%, 84.54%), and 2020 (12.29%, 87.71%). These results indicate that PFM% initially decreased, subsequently increased, while GE% initially rose followed by a slight reduction.

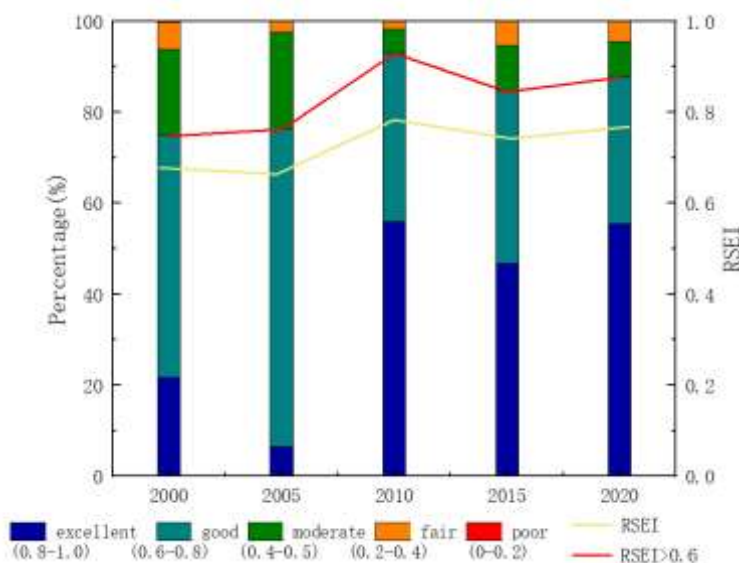


Figure 4 Proportional changes of ecological quality levels

Table 4. Areas and proportion changes of RSEI levels in different years

RSEI Level	2000		2005		2010		2015		2020	
	Area/km ²	Ptc/%	Area/km ²	Ptc/%	Area/km ²	Ptc/%	Area/km ²	Ptc/%	Area/km ²	Ptc/%
Critical (0-0.2)	523.75	0.22	56.25	0.02	53.75	0.02	165.25	0.07	220.25	0.09
Suboptimal (0.2-0.4)	14380.25	6.06	5701.5	2.40	4044	1.71	12339	5.21	10272.25	4.34
Marginal (0.4-0.6)	44808.25	18.88	50489.75	21.28	12535	5.29	24151	10.19	18630	7.86
Acceptable (0.6-0.8)	126283.25	53.21	165337.5	69.67	87694	37.00	89300.5	37.69	76603.75	32.33
Optimal (0.8-1)	51343.25	21.63	15721	6.62	132666.25	55.98	111009	46.85	131203	55.38

3.2. Spatial Auto-Correlation Analysis

3.2.1. Global Spatial Auto-Correlation

Using the fishnet tool in ArcGIS, grids of five spatial scales (3 km × 3 km, 4 km × 4 km, 6 km × 6 km, 7.5 km × 7.5 km, and 9 km × 9 km) were generated. The RSEI values for 2000–2020 were then sampled onto each grid scale, and the Moran's I indices were calculated accordingly.

Table 5 shows Moran's I indices computed at different scales from 2000 to 2020, and all corresponding z-scores exceeded 1.96, confirming significant spatial autocorrelation of RSEI across the study area. At this resolution, Moran's I

exhibited a unimodal temporal pattern, increasing during 2000–2010 before moderating from 2010–2020. In general, the Moran's I reflecting an enhancement of spatial clustering effect and indicating an increased spatial differentiation pattern in Guangxi's RSEI. As spatial scales increased, Moran's I values and corresponding z-scores decreased, demonstrating that increasing sampling grid sizes led to a higher degree of homogenization between grids. When grid sizes became excessively large, spatial auto-correlation diminished due to information loss within individual grids.

Table 5. Changes in Moran's I.

Scale	2000		2005		2010		2015		2020	
	Moran's I	z	p	Moran's I	z	p	Moran's I	z	p	Moran's I
3	0.826	154.56	0.000	0.848	213.73	0.000	0.869	158.87	0.000	0.841
4.5	0.814	91.12	0.000	0.834	145.61	0.001	0.845	104.36	0.000	0.833
6	0.809	86.34	0.000	0.822	114.72	0.001	0.845	78.40	0.000	0.837
7.5	0.801	65.17	0.000	0.817	84.46	0.001	0.829	62.012	0.000	0.818
9	0.803	51.44	0.000	0.817	73.07	0.001	0.822	51.494	0.000	0.811

3.2.2. Local Spatial Auto-Correlation

Spatiotemporal patterns of ecological quality were characterized by analyzing RSEI clustering via Local Indicators of Spatial Association (LISA) at a 3-km spatial resolution. Figure 5 reveals statistically non-significant areas predominantly concentrated in mountainous zones, contrasting

with significant high-high (H-H) clusters concentrated in the northeastern sector. From 2000 to 2005, H-H clusters exhibited scattered patterns. During 2010–2020, the area of H-H clusters notably expanded, indicating improved ecological environmental conditions. Low-low (L-L) clusters were principally concentrated around

Nanning city and regions adjacent to Guangdong Province. These areas corresponded to economically developed zones, reflecting

relatively poorer ecological quality associated with intensive urbanization.

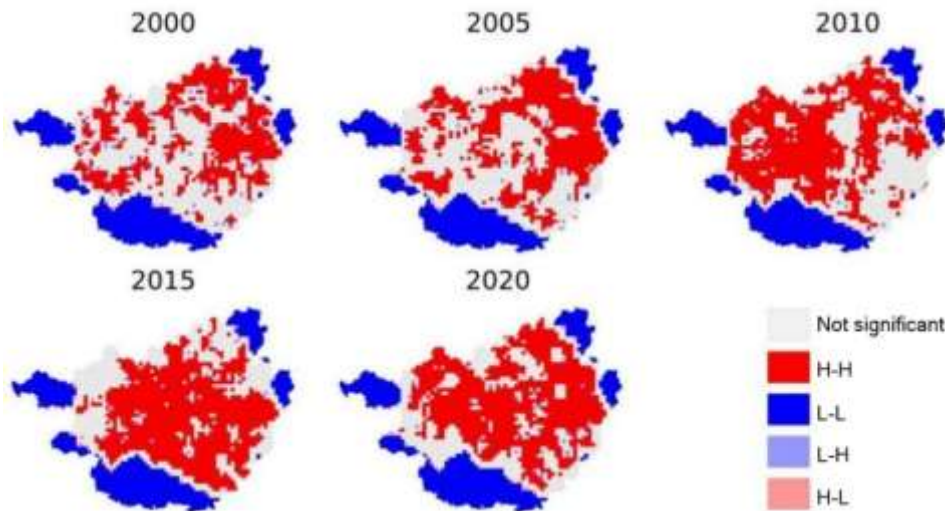


Figure 5. Local spatial auto-correlation of RSEI.

3.3. Driving Factors Analysis of RSEI

Table 6 reveals that all eight examined factors exerted significant effects on RSEI variations ($p < 0.001$). These factors include: elevation(X1), slope(X2), population density(X3), GDP(X4), annual precipitation (X5), distance to water bodies(X6), distance to roads(X7), distance to government location(X8). Elevation and slope emerged as the predominant factors influencing RSEI changes throughout the 2000-2020 period, with their explanatory capacity (q-

value) exhibiting a progressive increase over time. The q-values for elevation specifically, across the study years (2000, 2005, 2010, 2015, 2020), were 0.51, 0.54, 0.61, 0.64, and 0.63, respectively. Similarly, the slope factor's explanatory power increased correspondingly, showing values of 0.39, 0.44, 0.53, 0.54, and 0.59 for the same years. The underlying reason might be attributed to the relatively lower degree of human-driven development activities occurring in areas with lower elevations and gentle slopes.

Table 6. Explanatory power of driving factors on RSEI variations from 2000 to 2020.

	2000		2005		2010		2015		2020	
	p	q	p	q	p	q	p	q	p	q
X1	0.51	0.000	0.54	0.000	0.61	0.000	0.64	0.000	0.62	0.000
X2	0.39	0.000	0.44	0.000	0.53	0.000	0.54	0.000	0.58	0.000
X3	0.31	0.000	0.32	0.000	0.40	0.000	0.39	0.000	0.41	0.000
X4	0.29	0.000	0.32	0.000	0.38	0.000	0.32	0.000	0.23	0.000
X5	0.23	0.000	0.31	0.000	0.27	0.000	0.34	0.000	0.32	0.000
X6	0.33	0.000	0.35	0.000	0.34	0.000	0.35	0.000	0.33	0.000
X7	0.17	0.000	0.24	0.000	0.23	0.000	0.20	0.000	0.22	0.000
X8	0.21	0.000	0.21	0.000	0.21	0.000	0.22	0.000	0.18	0.000

The explanatory capability of population density increased steadily from 0.30 in 2000 to 0.42 in 2020, indicating intensified human influences on environmental quality. Conversely, GDP initially increased from 0.30 in 2000 to 0.39 in 2010, then

decreased notably to 0.23 by 2020, suggesting that economic development and construction activities gradually aligned with environmental protection considerations. Throughout the 20-year period, annual precipitation—facilitating vegetation

growth—exhibited fluctuations with an overall increasing explanatory effect. Likewise, the explanatory power of distances to water bodies and roads also fluctuated and increased, reflecting that rational and effective urban blue-green space planning significantly enhances urban ecological environments.

4. Discussion

4.1. Calculation of RSEI

Within investigation, the coefficient assigned to the first principal component (PC1) for RSEI computation in 2000 was comparatively reduced. Nevertheless, this deviation did not compromise the integrity of the overall findings. The implemented principal component analysis (PCA) methodology prioritized the effective characterization of ecological indicators. As shown in Table 3, PC1 presented positive loadings for the vegetation index and moisture index, indicating their positive contributions to ecological quality. Conversely, land surface temperature and dryness index displayed negative loadings, reflecting their adverse effects. In contrast, the loadings of WET, NDBSI, NDVI, and LST varied irregularly between positive and negative values in PC2, PC3, and PC4, contradicting actual ecological conditions. Thus, only PC1 reasonably represented RSEI and effectively interpreted ecological environmental quality without influencing the overall results.

Although the adopted method has shown its effectiveness in evaluating historical spatiotemporal variations of ecological quality, certain limitations should be further explored in future research. First, the RSEI-based ecological evaluation method primarily emphasized greenness, wetness, heat, and dryness indicators. However, ecosystems are complex and multidimensional systems involving diverse factors, including natural processes, socioeconomic development, and governmental management. Greenness (NDVI) and wetness (WET) indicators exerted positive influences on RSEI, whereas dryness (NDBSI) and heat (LST) indices had negative impacts. These findings align closely with previously reported results [34–36]. Moreover, greenness and dryness indicators exhibited stronger impacts compared to other indices.

Ecological environmental quality of water bodies is also an important issue in Guangxi; however, this study inadequately considered ecological quality in water and air environments. Future ecological evaluations should incorporate water and air quality more comprehensively. Due to the limited data sources used for RSEI in this study, subsequent research should employ a broader range of spatial datasets, such as GPP and LAOD.

4.2. Analysis of RSEI

In this research, elevation and slope positively influenced RSEI distribution with increasing significance over time, indicating that regions with higher elevation and steeper slopes, where development activities are difficult and human habitation is unsuitable, exhibited better ecological conditions. These findings were consistent with previous studies [37]. Economic growth and population increases inevitably exert environmental pressure, especially within urban centers. Nevertheless, following the introduction of ecological policies in China, the explanatory power of GDP regarding spatial variations in RSEI has decreased since 2010, demonstrating that economic growth has gradually shifted from sacrificing environmental quality.

Additionally, the positive driving effects of distances to water bodies and parks have increased, reflecting positive urban blue-green space construction practices that have improved urban ecological conditions to some extent. However, the GeoDetector method could not elucidate spatial associations clearly; hence, subsequent studies should further investigate the spatial impacts of various factors on Guangxi's RSEI by employing local regression analyses to better determine spatial-temporal variations in the direction and strength of these effects.

4.3. Policy recommendations

we propose the following integrated policy framework to enhance ecological governance in Guangxi: First, establish a provincial multi-indicator monitoring system that supplements current RSEI components (NDVI, WET, LST, NDBSI), air quality metrics (e.g., PM_{2.5}, aerosol optical depth), and biogeochemical proxies like Gross Primary Productivity (GPP), particularly for karst-coastal ecosystems. Second, implement strict zoning controls by designating high-elevation (>500 m) and steep-slope (>25°) areas

as "Ecological Conservation Redlines" with development prohibitions, coupled with reforestation incentives for marginal farmland on slopes $>15^\circ$ to leverage NDVI's 32–47% contribution to PC1 variance. Third, decouple economic growth from environmental pressure through green GDP accounting in performance evaluations and tax incentives for circular-economy industries, capitalizing on GDP's declining explanatory power over RSEI since 2010. Concurrently, optimize blue-green infrastructure (BGI) by mandating 15% minimum coverage in urban planning and restoring 100–500 m native-vegetation riparian buffers along major rivers to amplify WET's positive loading ($\beta = +0.68$). Finally, develop spatially-targeted governance using county-level RSEI anomaly maps generated via geographically weighted regression (GWR) to allocate ecological compensation funds dynamically, prioritizing regions where NDBSI exerts above-average negative impacts ($\beta < -0.71$). Implementation requires establishing a Guangxi Ecological Quality Collaborative Platform under the Department of Ecology and Environment to coordinate quarterly RSEI updates (using Sentinel-2/Landsat-9 and Google Earth Engine) and enforce cross-sectoral compliance, thereby balancing development and conservation in ecologically fragile interfaces while addressing methodological constraints.

5. Conclusions

Taking advantage of the GEE and MODIS imagery, this project quantifies the spatiotemporal trajectories of the ecological quality within Guangxi (2000–2020) by Remote Sensing Ecological Index (RSEI) Spatial heterogeneity patterns were heavily characterized.

The results showed that for the five historical remote sensing images (2000, 2005, 2010, 2015, 2020), all mean RSEI values were within the range of 0.6–0.8, with 8.477, 0.663, 0.782, 8.741, and 0.767, respectively, showing that Guixi's overall ecological quality was generally good. Ecological conditions gradually got better as they went from the middle parts to the surrounding areas. The H-H clusters were mostly concentrated in northeastern Guangxi, while L-L clusters were mainly distributed in Nanning City and areas close to Guangdong Province, which reflected the poorer ecological quality caused by more

intensive urbanization and economic development activities.

In terms of area changes among different RSEI categories, regions classified as "Critical" decreased by 303.5 km², and those classified as "Suboptimal" declined by 4,108 km². Moreover, the "Marginal" area decreased by 26,178.25 km², while the "Acceptable" area shrank by 49,679.5 km². Conversely, the "Optimal" ecological quality area significantly increased by 79,859.75 km², indicating a clear overall improvement in ecological conditions toward the "Optimal" category.

Elevation and slope emerged as predominant drivers governing RSEI dynamics during 2000–2020. Concurrently, population density demonstrated temporally escalating explanatory capacity across the study period.

Author Contributions: Yu Bai wrote the paper, Xiangling Tang and Wei Li directed the framework and conception of the paper. Tingjiang Tan, XueMei Zhong and Dujiang Long were responsible for the polishing of the article. All authors reviewed the manuscript and all authors agree to be accountable for all aspects of the work.

Acknowledgments: The authors gratefully acknowledge funding for this research and would like to thank. At the same time, the authors are grateful to the anonymous reviewers and editors for their input and constructive comments.

Funding: This research was funded by Key Research and Development Projects of Guilin Science and Technology Bureau, Guangxi, China in 2023 (Project No. 20230111-1) and the natural science foundation of China Guangxi (2020GXNSFAA297266).

Data Availability Statement: The raw data supporting the conclusions of this article will be made available by the authors, without undue reservation.

Conflicts of Interest: The authors declare no conflicts of interest.

References

1. Shuqing Zhao, Liangjun Da, Zhiyao Tang, Hejun Fang, Kun Song & Jingyun Fang. (2006). Ecological Consequences of Rapid Urban Expansion: Shanghai, China. *Frontiers*

- in Ecology and the Environment,4(7),341-346.
2. Weijun Shen, Jianguo Wu, Nancy B. Grimm & Diane Hope. (2008). Effects of Urbanization-Induced Environmental Changes on Ecosystem Functioning in the Phoenix Metropolitan Region, USA. *Ecosystems*, 11(1), 138-155.
 3. College of Environmental Science and Engineering, Nankai University, Tianjin, 300350, PR China, College of Environmental Science and Engineering, Nankai University, Tianjin, 300350, PR China, MOE Key Laboratory of Pollution Processes and Environmental Criteria, Nankai University, Tianjin, 300350, PR China, College of Environmental Science and Engineering, Nankai University, Tianjin, 300350, PR China, College of Environmental Science and Engineering, Nankai University, Tianjin, 300350, PR China & College of Environmental Science and Engineering, Nankai University, Tianjin, 300350, PR China. (2018). Urbanization-induced ecological degradation in Midwestern China: An analysis based on an improved ecological footprint model. *Resources, Conservation & Recycling*, 137, 113-125.
 4. Chen C, Nie P J, Huang F C, Fan D, Xiang L, Zeng J, Chen F W & Hu G X. (2024). Ecological Environment Quality Assessment and Driving Mechanism Based on Improved RSEI Model: A Case Study of Taojiang County, Hunan Province [J/OL]. *Bulletin of Soil and Water Conservation*, 44(03), 159-170. doi:10.13961/j.cnki.stbctb.20240528.002. (Chinese)
 5. Islam Abu Reza Md Towfiqul, Islam H.M. Touhidul, Shahid Shamsuddin, Khatun Mst Khadiza, Ali Mir Mohammad, Rahman M. Safiur... & Almoajel Alia M.. (2021). Spatiotemporal nexus between vegetation change and extreme climatic indices and their possible causes of change. *Journal of Environmental Management*, 289, 112505-112505.
 6. Andrew M. Coutts, Richard J. Harris, Thu Phan, Stephen J. Livesley, Nicholas S.G. Williams & Nigel J. Tapper. (2016). Thermal infrared remote sensing of urban heat: Hotspots, vegetation, and an assessment of techniques for use in urban planning. *Remote Sensing of Environment*, 186, 637-651.
 7. Xu H Q. (2013). Development and Application of Remote Sensing-based Ecological Index in Urban Areas [J]. *Acta Ecologica Sinica*, 33(24), 7853-7862. (Chinese)
 8. Hu K H & Zhang Z. (2021). Spatiotemporal Characteristics and Influencing Factors of Ecological Quality in Liuba County, Qinling Mountains, Shaanxi Province [J]. *Journal of Ecology and Rural Environment*, 37(06), 751-760. doi:10.19741/j.issn.1673-4831.2020.0884. (Chinese)
 9. Cao C, Yang G L, Suo X H, Liu T, An X W & Hu D. (2022). Analysis of Ecological Environment Change in Fuxin City Based on Remote Sensing Ecological Index [J]. *Journal of Northwest Forestry University*, 37(02), 200-207. (Chinese)
 10. Zhang J & Yang Y Q. (2019). Remote Sensing Evaluation of Ecological Condition Changes in the Pearl River Delta Urban Agglomeration [J]. *Journal of Northwest Forestry University*, 34(01), 184-191. (Chinese)
 11. Zhang Yi, She Jiyun, Long Xiangren & Zhang Meng. (2022). Spatio-temporal evolution and driving factors of eco-environmental quality based on RSEI in Chang-Zhu-Tan metropolitan circle, central China. *Ecological Indicators*, 144,
 12. Wu Y J, Zhao X S, Xi Y, Liu H & Li C. (2019). Integrated Assessment and Spatiotemporal Variation of Ecological Quality in Tibet from 2006 to 2016 Based on MODIS Data [J]. *Acta Geographica Sinica*, 74(07), 1438-1449. (Chinese)
 13. Xia QianQian, Chen YaNing, Zhang XueQi & Ding JianLi. (2022). Spatiotemporal Changes in Ecological Quality and Its Associated Driving Factors in Central Asia. *Remote Sensing*, 14(14), 3500-3500.
 14. Wang Y, Zhao Y H & Wu J S. Long-term Dynamic Monitoring of Ecological Quality in Urban Agglomerations Based on Google Earth Engine Cloud Computing: A Case Study of the Guangdong-Hong Kong-Macao Greater Bay Area [J]. *Acta Ecologica Sinica*, 40(23), 8461-8473. (Chinese)
 15. Jia Haowei, Yan Changzhen & Xing Xuegang. (2021). Evaluation of Eco-Environmental Quality in Qaidam Basin

- Based on the Ecological Index (MRSEI) and GEE. *Remote Sensing*, 13(22),4543-4543.
16. Kumar Lalit & Mutanga Onesimo. (2018). Google Earth Engine Applications Since Inception: Usage, Trends, and Potential. *Remote Sensing*, 10(10),1509-1509.
 17. Jiang M.(2022). Spatiotemporal Variation and Driving Factors of Ecosystem Service Functions in the Southwestern Karst Region [D]. Huazhong Agricultural University. doi:10.27158/d.cnki.ghznu.2022.000009.(Chinese)
 18. Liu F Y, Tian X G & He L.(2024). Ecological Environment Quality Assessment of Karst Coal Mining Area Based on RS and GIS: A Case Study of Panzhou City [J]. *China Mining Magazine*, 33(02),63-68.(Chinese)
 19. Jiao X M, Zhang B, Gao Y, Zheng M X, Zhou Y & Kuang W J.(2024). Ecological Environment Quality Evaluation in Karst Areas Using an Improved Remote Sensing Ecological Index [J]. *Bulletin of Surveying and Mapping*, 2024,(04),54-60. doi:10.13474/j.cnki.11-2246.2024.0410.(Chinese)
 20. Xu H Q.(2005). Study on Water Body Information Extraction Using Improved Modified Normalized Difference Water Index (MNDWI) [J]. *Journal of Remote Sensing*, (05),589-595.(Chinese)
 21. S. E. Lobser & W. B. Cohen.(2007). MODIS tasselled cap: land cover characteristics expressed through transformed MODIS data. *International Journal of Remote Sensing*, 28(22),5079-5101.
 22. Felizola A J F D & Mauricio L B ,A. B H.(2003). Spatial auto-correlation and red herrings in geographical ecology: Spatial auto-correlation in geographical ecology[J]. *Global Ecology and Biogeography*, 12(1):53-64.
 23. Boori Mukesh Singh, Choudhary Komal, Paringer Rustam & Kupriyanov Alexander. (2021). Spatiotemporal ecological vulnerability analysis with statistical correlation based on satellite remote sensing in Samara, Russia. *Journal of Environmental Management*, 285,112138-112138.
 24. Hui Yue, Ying Liu, Yao Li & Yang Lu.(2019). Eco-Environmental Quality Assessment in China's 35 Major Cities Based On Remote Sensing Ecological Index.. *IEEE Access*, 7,51295-51311.
 25. Pan Yang, Xinxin Zhang & Lizhong Hua.(2023). Analysis of Urban Ecological Quality Spatial Patterns and Influencing Factors Based on Remote Sensing Ecological Indices and Multi-Scale Geographically Weighted Regression. *Sustainability*, 15(9),
 26. Su Heng, Chen Yumin, Tan Huangyuan, Zhou Annan, Chen Guodong & Chen Yuejun.(2022). Estimating Regional PM2.5 Concentrations in China Using a Global-Local Regression Model Considering Global Spatial Autocorrelation and Local Spatial Heterogeneity. *Remote Sensing*, 14(18),4545-4545.
 27. Luo Meng, Zhang Shengwei, Huang Lei, Liu Zhiqiang, Yang Lin, Li Ruishen & Lin Xi.(2022). Temporal and Spatial Changes of Ecological Environment Quality Based on RSEI: A Case Study in Ulan Mulun River Basin, China. *Sustainability*, 14(20),13232-13232.
 28. Zhangyan Jiang, Alfredo R. Huete, Kamel Didan & Tomoaki Miura. (2008). Development of a two-band enhanced vegetation index without a blue band. *Remote Sensing of Environment*, 112(10),3833-3845.
 29. The Institute of Geography and Resources Science, Sichuan Normal University, Chengdu, 610068, China, Key Lab of Land Resources Evaluation and Monitoring in Southwest, Ministry of Education, Sichuan Normal University, Chengdu, 610068, China, The Institute of Geography and Resources Science, Sichuan Normal University, Chengdu, 610068, China, Key Lab of Land Resources Evaluation and Monitoring in Southwest, Ministry of Education, Sichuan Normal University, Chengdu, 610068, China, The Institute of Geography and Resources Science, Sichuan Normal University, Chengdu, 610068, China & Key Lab of Land Resources Evaluation and Monitoring in Southwest, Ministry of Education, Sichuan Normal University, Chengdu, 610068, China.(2019). Quantifying influences of natural factors on vegetation NDVI changes based on geographical detector in Sichuan, western China. *Journal of Cleaner Production*, 233,353-367.
 30. Liu Y S & Li J T.(2017). Geographic Exploration and Optimization Decision-making of Rural Poverty Differentiation

- Mechanism at County Level in China[J]. *Acta Geographica Sinica*,72(01),161-173.(Chinese)
31. Wu, Jiansheng,Li, Jiacheng,Peng, Jian,Li, Weifeng,Xu, Guang & Dong, Chengcheng. (2015).Applying land use regression model to estimate spatial variation of PM2.5 in Beijing, China.*Environmental Science and Pollution Research*,22(9),7045-7061.
 32. Jin-Feng Wang,Xin-Hu Li,George Christakos ,Yi-Lan Liao,Tin Zhang,Xue Gu & Xiao-Ying Zheng.(2010).Geographical Detectors-Based Health Risk Assessment and its Application in the Neural Tube Defects Study of the Heshun Region, China.*International Journal of Geographical Information Science*, 24(1),107-127.
 33. Jin-Feng Wang & Yi Hu.(2012). Environmental health risk detection with GeogDetector.*Environmental Modelling and Software*,33,114-115.
 34. Shan W ,Jin X & Ren J.(2019).Ecological environment quality assessment based on remote sensing data for land consolidation [J].*Journal of Cleaner Production*,239118126-118126.
 35. Gao Pengwen,Kasimu Alimujiang,Zhao Yongyu, Lin Bing,Chai Jinpeng,Ruzi Tuersunayi & Zhao Hemiao. (2020). Evaluation of the Temporal and Spatial Changes of Ecological Quality in the Hami Oasis Based on RSEI.*Sustainability*, 12(18), 7716-7716.
 36. Nie Xinran,Hu Zhenqi,Zhu Qi & Ruan Mengying.(2021).Research on Temporal and Spatial Resolution and the Driving Forces of Ecological Environment Quality in Coal Mining Areas Considering Topographic Correction.*Remote Sensing*,13(14),2815-2815.
 37. Zhou Jianbo & Liu Wanqing. (2022). Monitoring and Evaluation of Eco-Environment Quality Based on Remote Sensing-Based Ecological Index (RSEI) in Taihu Lake Basin, China. *Sustainability*, 14 (9),5642-5642.